J Mater Sci (2015) 50:6822–6832
DOI 10.1007/s10853-015-9239-y

Silicone dielectric elastomers based on radical crosslinked high molecular weight polydimethylsiloxane co-filled with silica and barium titanate

Adrian Bele[1] · George Stiubianu[1] · Cristian-Dragos Varganici[1] · Mircea Ignat[2] · Maria Cazacu[1]

Received: 16 April 2015 / Accepted: 4 July 2015 / Published online: 14 July 2015

Abstract A strategy, consisting in the use in tandem of two active fillers in different ratios with complementary effects: silica mainly as a reinforcing agent and barium titanate as dielectric permittivity enhancer, was proposed to optimize the electromechanical properties of the silicone elastomers. A high molecular mass polydimethylsiloxane-α,ω-diol (M_w = 642000 g mol^{-1}) was used as a matrix to prepare silicone composites which further were processed as films and crosslinked at high temperature. The morphological, thermal, and moisture behaviors of the films were studied by adequate techniques. The mechanical properties were estimated on the basis of normal and cyclic stress–strain curves. Dielectric spectra were recorded in the frequency range of 1–10^6 Hz at normal temperature. The voltages generated by a mechanical impulses created by falling of a metal ball of 7.1 g from a height of one hundred millimeters on the surface of the films placed between two electrodes ranged between 28.4 and 157.3 V mm^{-1}.

Electronic supplementary material The online version of this article (doi:10.1007/s10853-015-9239-y) contains supplementary material, which is available to authorized users.

✉ Maria Cazacu
mcazacu@icmpp.ro

[1] "Petru Poni" Institute of Macromolecular Chemistry, Aleea Gr. Ghica Voda 41A, 700487 Iasi, Romania

[2] National Institute for Research and Development in Electrical Engineering ICPE-CA, 313 Splaiul Unirii, 030138 Bucharest, Romania

Introduction

Energy-harvesting technologies aiming the conversion of different energy forms (light, thermal, mechanical, etc.) [1] from the natural sources such as wind, waves, or animal movements into electrical energy are attracting a high interest in the scientific community especially in the last 20 years [2, 3]. One way to convert the mechanical energy into electrical one is to use high reversible deformability of the dielectric elastomers. Among this class of materials, silicones attract great interest because of their high elasticity and weather resistance [4–8]. A drawback of silicones is their low dielectric permittivity (in the range of 2.5–3.0); many studies thus aim to improve this parameter to enable them maintain good mechanical properties. The unique molecular structure and chemistry of the silicone polymers permit their formulations to be able to meet the requirements of a specific application. Different strategies have been used to improve the dielectric properties [9], but the most promising one is the incorporation of filler particles with high dielectric permittivity, such as ceramic fillers (e.g., barium titanate, titanium dioxide, calcium copper titanium oxide, lead zirconate, etc.) [10–14]. The dielectric relaxation of the crystallites embedded into the polymer matrices was studied [15, 16], and the principal role of the interface states on the border polymer-crystallites was established in defining the corresponding dielectric features. Barium titanate, a ferroelectric crystal with high dielectric strength, is widely used for this purpose [17–20]. The effects of barium titanate ($BaTiO_3$) nanoparticles on electric and mechanical properties are extensively studied, and it was found that the dielectric constant of nanocomposites significantly increases with the increasing $BaTiO_3$ concentration, whereas volume resistivity decreases continuously [21]. However, while the

thermal stability of the composites in which it is incorporated increases, the mechanical properties, i.e., tensile strength and elongation at break deteriorate as BT content increases due to no reinforcing nature of BT [22]. On the other hand, the effective reinforcing effect (increases in tensile strength, tear resistance, compression set, and good dynamic properties besides anti-aging and anti-friction) of the nanosilica on the silicone rubber is well known [23, 24]. Depending on the silica content, the strength of the silicones could be significantly increased. However, with the addition of silica as filler, an increase in stiffness, undesired in electromechanical application, occurs simultaneously along with the resistance to fracture. Therefore, a compromise must be made between these two features.

Continuing our efforts to obtain silicone elastomers with optimized electromechanical properties [11, 25–28], in this paper, we addressed the working strategy consisting in the original combination of two active fillers with complementary effects: silica, as a reinforcing filler and barium titanate, both from commercial sources, to increase the dielectric permittivity of the composites obtained. In addition, the uniqueness of our approach consists in the use of a matrix of a polydimethylsiloxane of high molecular weight ($M_w = 642000$ g mol^{-1}) and its curing by a radical mechanism, which takes place at high temperature and pressure. The crosslinking pattern is different from that used in the majority of cases reported in the literature to stabilize the dielectric silicone elastomers for which, in general, commercial silicone kits with vulcanization by condensation of the chain ends with a tri- or tetrafunctional crosslinking agent are used [5, 25, 29, 30]. The system reported here rather resembles the curing by hydrosilylation, but it is applicable only in case of relatively low molecular weight polysiloxanes, with more flexibility to ensure access to each other functional groups (Si–H and Si–CH=CH$_2$) [27, 31, 32]. The films obtained by us are robust, easy to handle, and useful in tougher conditions. The effects of filler's presence and their amounts embedded into a polysiloxane matrix of high molecular weight on the mechanical properties and dielectric behavior were studied. Also, preliminary estimations of the ability of the resulted materials to convert mechanical energy into electric one were made on an in-house setup based on direct piezoelectric effect without previous polarization.

Materials and methods

Materials

The polymeric matrix, polydimethylsiloxane-α,ω-diol (PDMS), was obtained by bulk polymerization of octamethylcyclotetrasiloxane catalyzed by H_2SO_4, at room temperature (RT), according to procedure described in Ref. [33]. A small percentage of vinyl-substituted cycle (3 wt% heptamethylvinylciyclotetrasiloxane, ([$(CH_3)_2SiO]_3$[$C_2H_3(CH_3)SiO$]), was added. The polymer was purified by repeated washing with slight alkaline solution and then with water, until a neutral pH is attained. Then, the polymer was devolatilized in vacuum at 180 °C to remove water and low molecular weight siloxanes. The molecular mass, as was evaluated by gel permeation chromatography using chloroform as eluent, was $M_w = 642000$ g mol^{-1} ($M_n = 438000$ g mol^{-1}), $d = 1.00$ g cm^{-3}, and dielectric permittivity $\varepsilon' = 2.9$. Fumed silica—Aerosil 380 (Degussa)—with 100 % purity, specific surface area: 380 m^2 g^{-1}, particle diameter in the range: 3–15 nm, $d = 2.2$ g cm^{-3}, tapped density of around 50 g l^{-1}, dielectric permittivity: $\varepsilon' = 3.9$; and barium titanate, $BaTiO_3$, (Fluka AG), BT, m.p.: 1625 °C, particle size: <3 μm, $d = 6.08$ g cm^{-3}, dielectric permittivity: $\varepsilon' = 1700$ at RT were dried in vacuum at 100 °C and hydrophobized by treatment with dimethylcyclosiloxanes mixture in vapor state, 2,4-Dichlorobenzoyl peroxide as a paste 50 wt% in silicone oil, having a critical temperature: 60–70 °C and set-cure temperature in the range 115–150 °C.

Measurements

Gel permeation chromatographic analysis, GPC, was carried out on a PL-EMD 950 Evaporative Mass Detector instrument using $CHCl_3$ as eluent, after calibration with standard polystyrene samples. The obtained thick films were cryo-fractured, and the cross-sectional surface was examined using an environmental scanning electron microscope (ESEM) type Quanta 200, operating at 30 kV with secondary electrons in low vacuum mode. Stress–strain measurements were performed on TIRA test 2161 apparatus, Maschinenbau GmbH Ravenstein, Germany, on dumbbell-shaped cut samples with dimensions of 50 × 8.5 × 4 mm. Measurements were run at an extension rate of 20 mm min^{-1}, at RT. All samples were measured three times, and the averages of the obtained values were taken into consideration as final values. The acquired data were processed using MatLab software. Cyclic tensile stress tests were performed on the similar samples between 2 and 100 % strain. The maximum force applied was tensile stress value as determined by previous test. Five stretch–recovery cycles were registered. The stationary time at minimum and maximum applied stresses was 5 s. Novocontrol setup (Broadband dielectric spectrometer Concept 40, Germany), integrating an ALPHA frequency response analyzer and a Quatro temperature control system, was used to investigate the dielectric properties of the

polymer composites over a broad frequencies window, 10^0–10^6 Hz, at RT. The bias voltage applied across the sample was 1.0 V. Samples having thicknesses in the 0.5–1 mm range were placed between gold-plated round electrodes, the upper electrode having a 20 mm diameter. Differential scanning calorimetry measurements, DSC, were conducted on a DSC 200 F3 Maia (Netzsch, Germany). A mass of 10 mg from each sample was heated in pressed and pierced aluminum crucibles from −150 to 50 °C at a heating rate/cooling rate of 10/−10 °C min^{-1} and under nitrogen flow as inert atmosphere at a flow rate of 50 mL min^{-1}. The temperature against heat flow was recorded. The baseline was obtained by scanning the temperature domain of the experiments with an empty pan. The enthalpy was calibrated with indium according to standard procedures. Water vapor sorption capacity of the film samples was measured by means of the fully automated gravimetric analyzer IGAsorp supplied by Hiden Analytical, Warrington (UK). The measurements were performed at RT (~25 °C) in the 0–90 % relative humidity range (Fig. S3). A step of humidity change of 10 wt% and pre-established equilibrium time between 10 and 30 min were used. The samples were dried previously in flowing nitrogen (250 mL min^{-1}) until a constant weight was achieved. An ultrasensitive microbalance measures the weight change as the humidity is modified in the sample chamber at a constant regulated temperature. The measurement system is controlled by IGASORP Windows™-based software package. Harvesting experiments (voltage recording) were performed using a memory oscilloscope, Tektronix DPO 4032 (350 MHz, 2.5 GS s^{-1}), as was already described in Refs. [11, 23].

Preparation of the composites and films formation

Previously hydrophobized silica nanoparticles and barium titanate of different percentages were stepwise incorporated in small portions into the PDMS by mechanical mixing in a Janke–Kunkel laboratory mixer equipped with double palettes and cooling mantle, according to Table 1. The homogenization was finalized on a rampart, where the crosslinking catalyst (2 wt% 2,4-dichlorobenzoyl peroxide) was also added [33]. To obtain crosslinked films, small amounts of each mixture (~10 g) were put as a round blob of material inside frame (1 × 70 × 70 mm) mounted between two stainless steel plates (1 × 100 × 100 mm) and pressed with a manual press. Afterward, this assembly was heated at 120 °C for 1 h when crosslinking occurs. Then, the films peeling off from the substrate were post-heat treated by maintaining at 150 °C for 10 h in air stream for devolatilization. These films were used to investigate some of the properties of interest for the target application.

Table 1 Recipes to obtain desired elastomers (added catalyst: 2 wt% 2,4-dichlorobenzoyl peroxide)

Sample	Silica (wt%)	Barium titanate (wt%)
S0B0	0	0
S10B0	10	0
S10B5		5
S10B15		15
S15B0	15	0
S15B5		5
S15B15		15
S30B0	30	0
S30B5		5
S30B15		15

Results and discussion

A polydimethylsiloxane-α,ω-diol of high molecular mass (M_w = 642000 g mol^{-1}) was used as a matrix to prepare silicone composites. Two fillers, silica and barium titanate, were incorporated in different ratios (Table 1) within the polymer to improve its properties, each of them having a specific role. Thus, while the silica addition aims to improve the mechanical properties, the ceramic material should lead to increased dielectric permittivity. Both fillers were previously surface hydrophobized by treating with dimethylcyclosiloxanes mixture in vapor state. The composites formulated with different percentages of both fillers were processed as films with dimensions of 70 × 70 × 1 mm, and stabilized by radical curing initiated by 2,4-dichlorobenzoyl peroxide at 120 °C in a press. At high temperature, the peroxide decomposes to form free radicals that attack preferably vinyl groups, leading to continuous free radical chain reactions. Under such conditions, the crosslinking occurs by the formation of the alkylene (ethylene, propylene) interchain bridges along the siloxane backbone [34] (Fig. 1).

Morphology

The distribution of the fillers within the polymeric matrix was evaluated by SEM examination of the cryo-fractured cross-sectional surface. The SEM images of the samples filled with silica only, taken with the resolution according to Fig. 2, reveal a good dispersion of these nanoparticles not being identified as individual or agglomerated silica nanoparticles either at 10 or at 30 wt% content (sample S10B0—Fig. 2d, S15B0—Fig. 2g and S30B0—Fig. 2j). Instead, in the samples in which barium titanate was incorporated, aggregates thereof with large dimensional

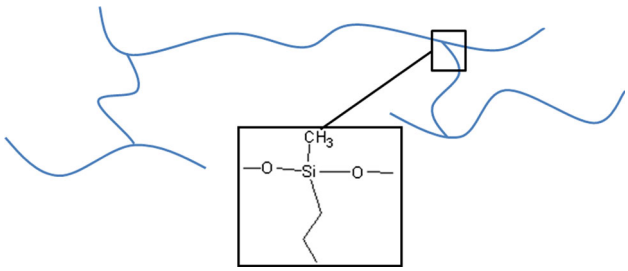

Fig. 1 Chain crosslinking pattern

dispersion from a few micrometers corresponding to ex situ dimensions of the barium titanate (Fig. 2a, b) to 50–60 μm (Fig. 2f–l) can be seen. It is presumed that the aggregation occurs during the hydrophobization treatment due to the high incompatibility between the strong hydrophobic dimethylcyclosiloxane and hydrophilic barium titanate, which is not soluble in water but disperses well in it. As a result, there is a natural tendency of the particles to agglomerate at the expense of their coverage with a hydrophobic coating. It seems that this method is not optimal for the hydrophobization of barium titanate. It is assumed that the use of a silane-coupling agent such as alkyltrialkoxysilane or hexamethyldisilazane would be more appropriate in order to maintain a good dispersion of the polar filler within a nonpolar matrix.

Mechanical behavior

Stress–strain curves were recorded (Fig. 3a) at RT and atmospheric humidity.

The main parameters estimated on the basis of these curves are compiled in Table 2.

Due to the compatibility and reinforcing effects of silica nanoparticles, the mechanical properties were enhanced with the increasing incorporated amounts. Thus, the ultimate tensile strength increases from 0.15 MPa for pure crosslinked silicone to 5.03 MPa when 30 wt% silica was incorporated (Table 2). However, the increases in elongation are modest, from 162 % for S0B0 to 272, 328, and 326 % for the elastomers containing 10, 15, and 30 wt% SiO_2, respectively. As a result, the Young's modulus significantly increased, from 0.30 MPa for pure crosslinked silicone to 4.78 MPa for elastomer filled with 30 wt% silica. When the second filler, barium titanate, was added, due to its lower compatibility with silicone matrix and aggregates' formation during the hydrophobization and incorporation procedures in polymeric matrix by mechanical mixing, a deterioration in the values of both ultimate tensile stress and elongation for the series S10 and S15 containing lower silica content is registered, while the Young's modulus continues to increase. This growth is not just of the same magnitude as that induced by incorporating increasing amounts of silica but also generally occurs systematically—as BT content increases from 0 to 15 %—in all the three series, S10, S15, and S30, from 0.86 to 0.89, from 1.33 to 2.10, and from 4.78 to 8.25 MPa, respectively, as suggested by graphical presentation in Fig. 4.

In order to evaluate mechanical fatigue resistance, cyclic stress–strain tests were performed, with five cycles being performed for each sample until 100 % elongation from the initial length, at RT and atmospheric humidity (Fig. 3b). After the first cycle, all samples show a big hysteresis loop which disappears, due to the rearrangements of polymeric chains which undergo elongation, also known as Mullins effect [35]. The shape of the cyclic stress–strain curves reveals that the incorporation of low percentage of silica does not significantly affect the elastic properties of silicones. These are also not drastically affected by adding barium titanate to the composites containing 10 and 15 wt% silica. Instead, in the case of the composites containing 30 wt% silica and different percentages of barium titanate, the viscoelastic loss is manifested by the presence of visible hysteresis loops on the stress–strain curves. By the incorporation of the silica only (i.e., samples S10B0, S15B0, S30B0), the elastic region (where Hook's law can be applied) significantly decreases from 32.6 % in pure crosslinked PDMS to 19.4, 15.6, and 12 % when 10, 15, and 30 wt% silica, respectively, were added (Table 2). This is a consequence of the limitations in the polymer chains movement due to the physical bond changes that occurred within the strained material [36]. The contribution of the barium titanate to the viscoelastic loss is much lesser. The maximum limits of pure elastic strain decreased from 19.4 to 14.6, from 15.6 to 10.6, and from 12.1 to 9.9 %, when 15 wt% barium titanate was incorporated into the samples of the three series, already containing 10, 15, and 30 % silica, respectively.

Dielectric spectroscopy

Dielectric spectra were also recorded at RT in the frequency range 1–10^6 Hz (Fig. 5) with the intention of having increased dielectric permittivity values, while limiting the dielectric loss to be at low level, which creates prerequisites for applying a low voltage for actuation or for more energy that could be harvested.

As can be seen, even the addition of silica only leads to a slight increase of the dielectric permittivity from 3.02 for pure matrix to 3.45 and 3.48 with the additions of 15 and 30 wt% silica, respectively. When barium titanate was added, the dielectric permittivity increases as the filler content is increased from 5 to 15 wt% (Table 2; Fig. 6). The highest value, 4.26, was registered for the sample S30B15 with the highest amounts of the two fillers.

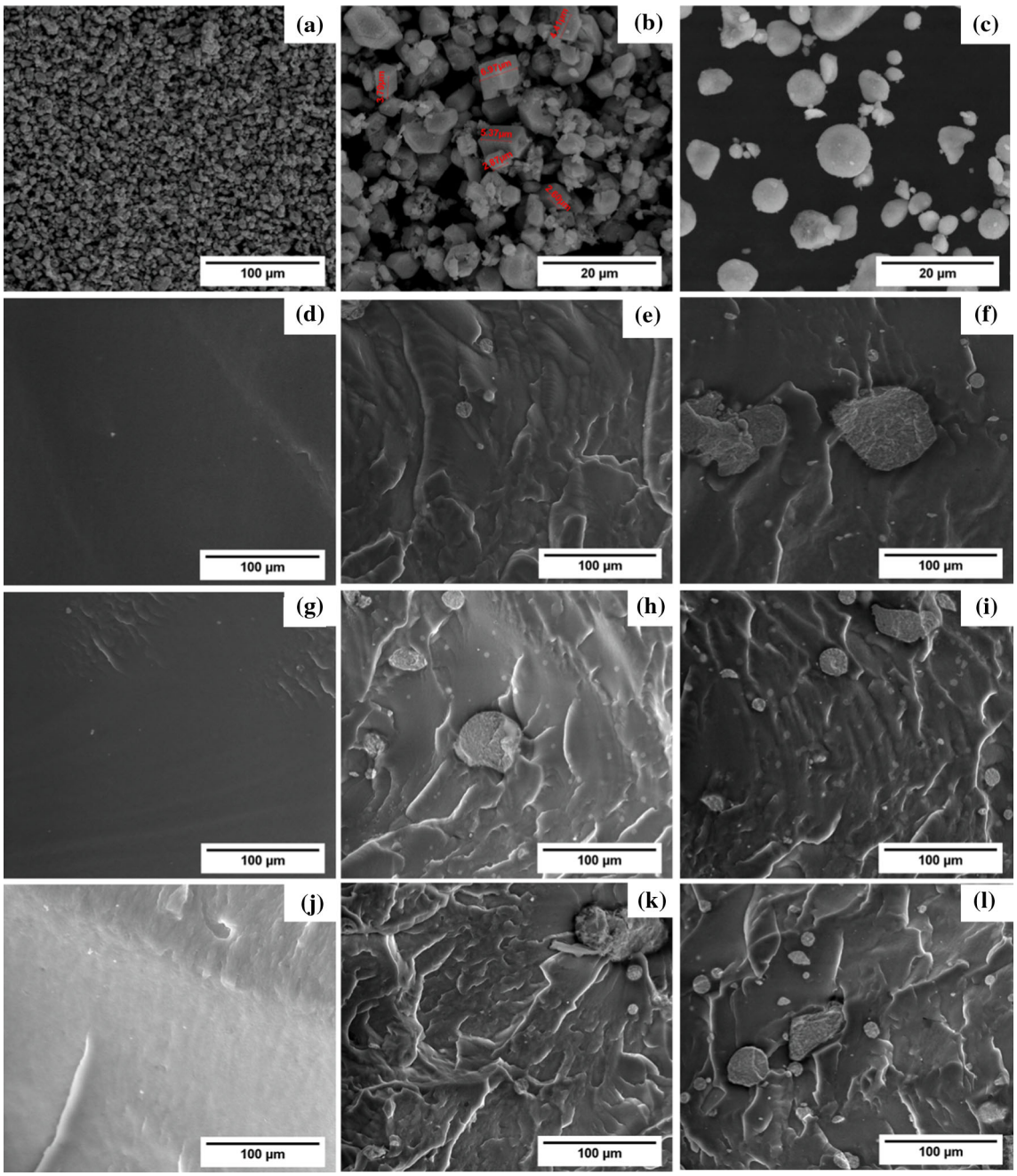

Fig. 2 SEM images of **a**, **b** raw commercial barium titanate, **c** surface-treated commercial barium titanate, and **d** S10B0, **e** S10B5, **f** S10B15, **g** S15B0, **h** S15B5, **i** S15B15, **j** S30B0, **k** S30B5, **l** S30B15 in cryo-fractured cross-sectional surfaces

The increase in the dielectric permittivity of the composite, as the added amount of barium titanate increases, is an expected one, at least from the perspective of volume-fraction average model:

$$\varepsilon_{\mathrm{ff}} = \varphi_{\mathrm{p}}\varepsilon_{\mathrm{p}} + \varphi_{\mathrm{c}}\varepsilon_{\mathrm{c}} + \varphi_{\mathrm{s}}\varepsilon_{\mathrm{s}} \quad (1)$$

where the subscripts p, c, and s refer to the polymer, the ceramic phase, and silica, respectively; and φ is the volume fraction of the constituents. When an electric voltage is applied, positive and negative charges appear at the surface of the polar particles dispersed within the continuous phase. Thus, the particles behave as dipoles, which align head-to-tail in the direction of the electric field, and the polarization leads to increased capability of the prepared dielectric materials to store energy [37]. Logically speaking, by increasing the volume fraction of the component with the highest dielectric permittivity ($\varepsilon'_{\mathrm{BT}} = 1700$ at RT), the dielectric permittivity of the composite should

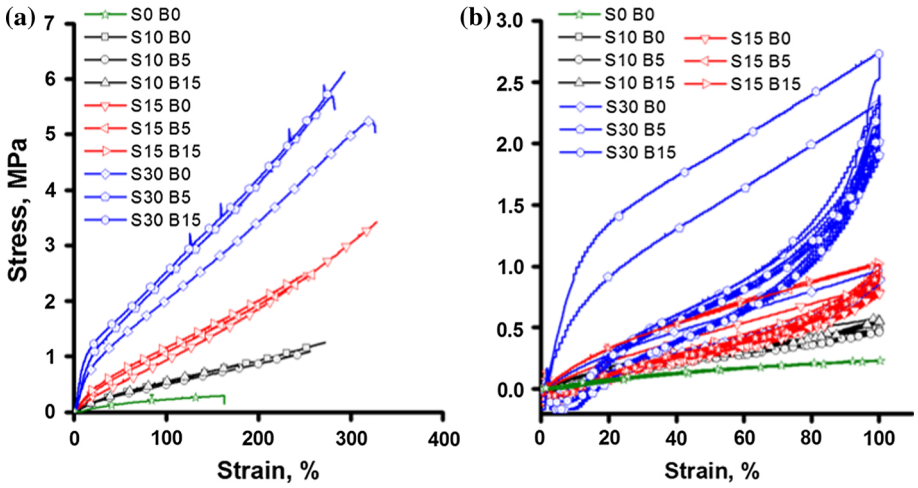

Fig. 3 Normal (**a**) and cyclic (**b**) stress–strain curves recorded at RT and atmospheric humidity

Table 2 Relevant mechanical, dielectric, and electromechanical data for as-prepared silicone composites

Sample	d (mm)[a]	σ (MPa)[b]	ε (%)[c]	σ_{el} (MPa)[d]	ε_{el} (%)[e]	E (MPa)[f]	ε'[g]	ε''[h]	U_{vv} (V)[i]	U_{vv}/d (V mm^{-1})[j]
S0B0	1.60	0.15	162	0.1021	32.6	0.30	3.02	0.01	8	5.0
S10B0	0.88	1.25	272	0.1707	19.4	0.86	3.41	0.01	25	28.4
S10B5	0.89	1.09	255	0.0439	5.4	0.81	3.67	0.01	140	157.3
S10B15	0.91	0.81	178	0.1340	14.6	0.89	3.95	0.01	90	98.9
S15B0	0.84	3.41	328	0.2140	15.6	1.33	3.48	0.01	70	83.3
S15B5	0.91	2.50	259	0.2639	13.7	1.91	3.66	0.02	49	53.8
S15B15	0.96	2.45	247	0.2337	10.6	2.10	4.09	0.02	98	104.1
S30B0	0.82	5.03	326	0.5030	12.1	4.78	3.45	0.01	76	92.7
S30B5	1.01	5.44	282	0.7445	12.1	5.85	3.89	0.01	61	60.4
S30B15	0.93	6.13	292	0.9690	9.9	8.25	4.26	0.01	37	39.8

[a] Film thickness

[b] Stress at break

[c] Elongation at break

[d] Stress at the upper limit of elasticity

[e] Strain at the upper limit of elasticity

[f] Young's modulus (calculated at 15 % strain)

[g] Dielectric permittivity at 10 Hz

[h] Dielectric loss at 10 Hz

[i] Harvested energy, expressed as a peak to peak voltage

[j] Harvested energy reported to the film thickness, expressed as a peak to peak V mm^{-1}

increase. However, the values obtained by this theoretical approach are very much higher than experimental ones (Table S1; Fig. S2). In fact, the prediction of dielectric permittivity value by this way has been already disproved by other theoretical [38] and experimental [39] studies. Instead, the experimental values better fit the theoretical ones obtained using other models, such as Maxwell–Garnett [40], Bruggeman [40, 41], and Lichtenecker–Rother [41–48] (see SI) as shown in Fig. 7.

An interesting aspect is that, the dielectric permittivity remains almost stable over the entire range of frequencies. This might be ascribed to high stiffness matrix limiting pole orientation even at low frequencies. Dielectric loss values are low for all samples; thus, the used fillers do not affect the insulating properties of PDMS-based elastomers. The negative values on some of dielectric loss curves recorded around 10^3 and over 10^5 Hz frequencies are due to resolution limits of the dielectric spectrometer.

DSC analysis

In order to see how the incorporation of the fillers affects the thermal transitions of the PDMS in composites, DSC curves were recorded in the range of −150 to +50 °C. It

was observed (Fig. S4) that these do not vary significantly, but only by a few degrees with plus or minus from the reference sample values. Thus, the operating temperature window for composites does not change from that known for the silicones. Absolute heat capacity values determined on the basis of DSC curves (Fig. S4; Table 3) were used to estimate the crosslinking density according to the procedure described in the literature [49–51]. The following equation was used:

$$\rho_c = (C_p^i - C_p^0)/C_p^0 \quad (2)$$

with C_p^i being the heat capacity of the polymer network at a given crosslinking density [1, 52] and C_p^0 the heat capacity of the noncrosslinked polymer. The heat capacity is a measure which energetically characterizes only segmental chain mobility in the polymer matrix. Polydimethylsiloxanes have T_g around −123 °C, while data from DSC analysis for the crosslinked samples show T_g values around this same temperature (−123 °C) (Fig. S3). Therefore, the heat capacity for this transition is used for calculating the crosslinking density value, using Eq. (2), for each of the prepared samples. The results are illustrated in Table 3.

The crosslinking degree decreases when silica particles are introduced in the composition of the silicone elastomers (from 0.328 mol cm^{-3} for S0B0 to 0.196–0.246 mol cm^{-3} by incorporating silica), and this leads to a small decrease of T_g, with 1–3 °C in comparison with the pure crosslinked PDMS, S0B0. The surface of the silica particles is treated with octamethylcyclotetrasiloxane, and therefore, these particles are not acting as crosslinking centers, but occupy the free volume between the siloxane polymer chains and interact with these only by physical interactions. However, the introduction of 15 wt% barium titanate nanoparticles in the formulation of the elastomers seems to lead to small increases of crosslinking density (i.e., to 0.260, 0.287, and 0.260 mol cm^{-3} for the samples S10B15, S15B15, and S30B15, respectively) compared with samples containing silica only, but not up to the level of pure siloxane polymer. Unfortunately, it cannot establish any correlation between the crosslinking degree and the mechanical or dielectric characteristics due to the complexity of the material induced by the presence of the two fillers.

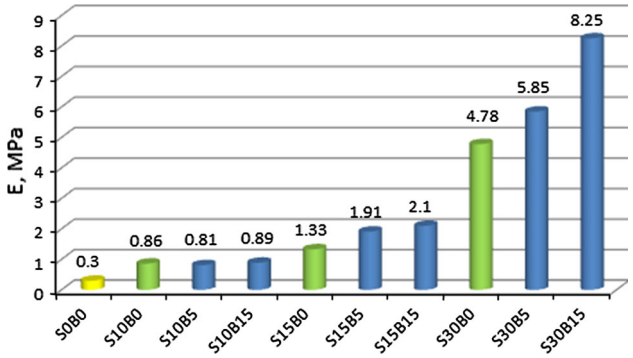

Fig. 4 Evolution of elastic modulus (determined at 15 % strain) with the filler's content

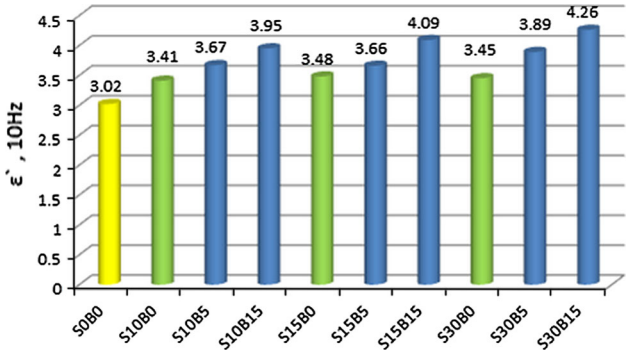

Fig. 6 Comparative values of the dielectric permittivity at 10 Hz for the samples containing the two co-fillers in different ratios

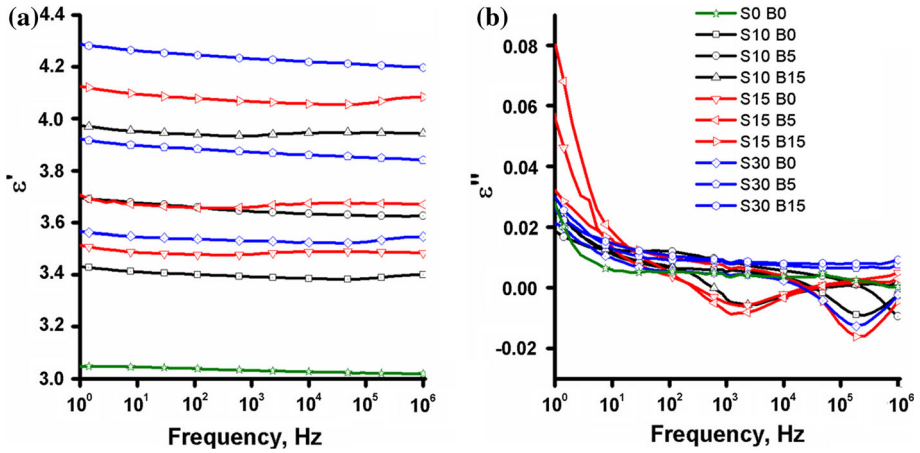

Fig. 5 Dielectric measurements: **a** dielectric permittivity; **b** dielectric loss; the *symbols* have the same meaning for both graphs

Vapor sorption capacity

The amount of humidity adsorbed by the dielectric can lead to failure when a voltage is applied; conductive pathways can form, and dielectric breakdown suddenly appears. For this reason, the moisture behavior of the samples was investigated by recording water vapor sorption isotherms at RT (~25 °C) in the 0–90 % relative humidity range (Fig. S3). The maximum sorption values range between 0.33 and 0.89 wt% indicating the existence of hydrophobic materials. A maximum sorption capacity of 0.57 wt% was recorded for the pure crosslinked silicone matrix, while very slight increases only can be noticed for some of the samples filled with silica (0.7, 0.66, and 0.75 wt%) or silica and barium titanate (most of them around 0.8 wt%) but without a logical variation (Table 3).

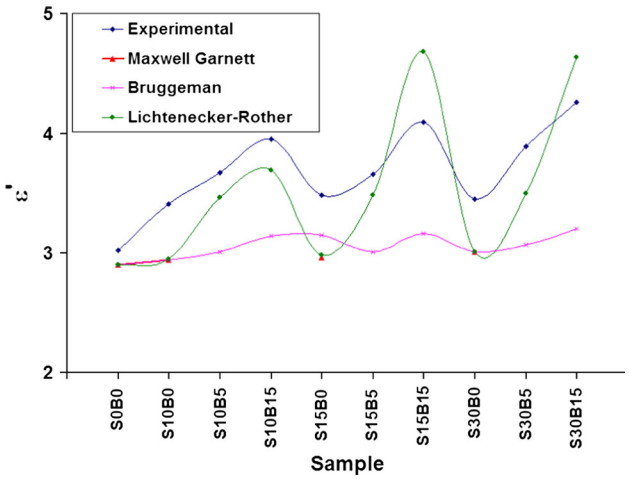

Fig. 7 Plot of experimental dielectric permittivity values compared to those of theoretical estimated ones using different models

Energy-harvesting measurements

The capacity of the sample to convert the mechanical energy into electrical one, sought as ultimate features, was estimated by means of a setup similar to that described by us in Ref. [11], which involved measuring peak-to-peak voltages generated by a mechanical impulse created by falling of a metal ball of 7.1 g from a height of 100 mm on the surface of the elastomeric films placed between two electrodes (Fig. 8).

The dynamic parameters used for these experiments are as follows:

– speed at contact with the elastomeric membrane, υ:

$$v = \sqrt{2gh} = \sqrt{2 \times 9.8 \times 0.1} = 1.4\,(\mathrm{m/s}) \quad (3)$$

– mechanical impulse, p:

$$p = mv = 9.94 \times 10^{-3}\,(\mathrm{Ns}) \quad (4)$$

– kinetic energy in contact, E:

$$E = \frac{mv^2}{2} = 6.96 \times 10^{-3}\,(\mathrm{J}) \quad (5)$$

– the microforce, F:

$$F = \frac{E}{h} = 0.0696\,(\mathrm{N}). \quad (6)$$

Compared with the existing results [29, 53–55], the amounts of energy harvested, expressed as a peak-to-peak voltage for all samples (Table 2), indicate good values ranging between 25 and 140 V. As films of different thicknesses were measured, the peak-to-peak voltages have been reported for the film thicknesses in order to have better comparison of the samples to each other. It seems,

Table 3 Thermal and moisture sorption data

Sample	DSC data		Weight (% d.b.)[b]
	Heat capacity, C_p (J g^{-1} K^{-1})[a]	Crosslinking density ρ_c' (mol cm^{-3})	
PDMS	0.073	–	–
S0B0	0.097	0.328	0.57
S10B0	0.058	0.205	0.70
S10B5	0.061	0.164	0.36
S10B15	0.092	0.260	0.52
S15B0	0.091	0.246	0.66
S15B5	0.088	0.205	0.82
S15B15	0.052	0.287	0.33
S30B0	0.066	0.096	0.75
S30B5	0.087	0.191	0.89
S30B15	0.054	0.260	0.86

[a] Crosslinking density

[b] Maximum water vapor sorption capacity reported to the dry mass

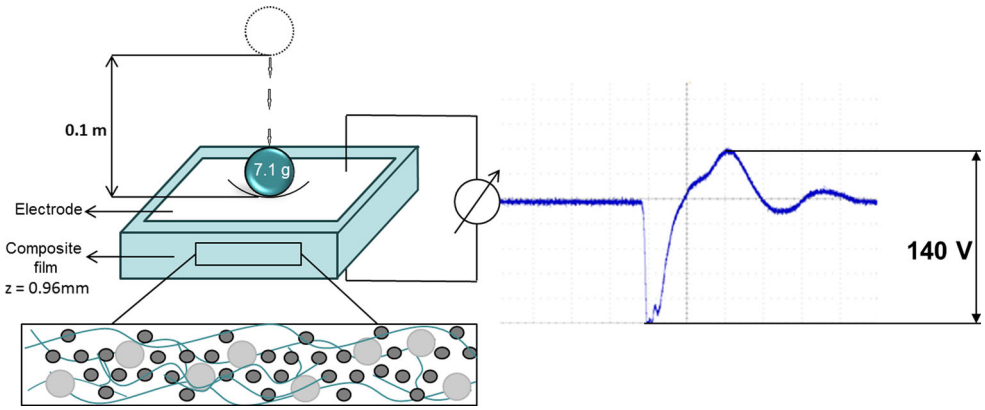

Fig. 8 Setup for the energy-harvesting measurements and an illustrative signal registered for the sample S10B5 (see Fig. S5 for the other samples)

besides dielectric permittivity values induced by incorporations of the silica and barium titanate contents, Young's modulus also has a great influence. Thus, the sample S10B5 (10 wt% silica and 5 wt% barium titanate) having the lowest value of Young's modulus (0.81 MPa) among all the composites showed the highest harvested energy value, i.e., 157.3 V mm^{-1}, although the dielectric permittivity value is 3.67 only.

Conclusions

A series of silicone elastomer samples have been prepared by incorporations of two fillers, silica and barium titanate, each of which has different roles within a high molecular mass polydimethylsiloxane-α,ω-diol, followed by a peroxide crosslinking. By incorporating silica, Young's modulus strongly increased, as expected, but there was also a very slight increase in the dielectric permittivity value. However, with the addition of the second filler, barium titanate, while the dielectric permittivity more significantly increases, as expected, reaching 4.26 in value (at 15 wt% barium titanate and 30 wt% silica loadings), and the obtained values reasonably fit those estimated on the basis of several theoretical models, unacceptable results are registered both in tensile stress and elongation values in the series with lower amounts of silica (S10 and S15), due to lower compatibility of ceramic filler with silicone matrix and the formation of aggregates. Cyclic stress–strain tests revealed that the elastic properties of the resulted elastomers are not significantly affected by incorporation of barium titanate, but they are rather influenced by the silica content. The dielectric permittivities of all prepared samples remain almost stable over the entire range of frequencies. Dielectric loss values are low for all the samples. The incorporations of the silica and barium titanate do not significantly affect the thermal transitions and moisture sorption of the composites. Instead, by incorporating silica, the crosslinking degree decreases as was determined on the basis of DSC curves, while with co-addition of barium titanate, some of this loss is recovered, but not to the level found in pure crosslinked silicones. The preliminary harvesting tests reveal promising results, with the best value, 157 V mm^{-1}, being obtained in the case of the sample, which has the lowest Young's modulus among the prepared composites, 0.81 MPa, and a dielectric permittivity value of 3.67. Thus, starting from the chosen polymer matrix and crosslinking system and considering the harvested output energy as ultimate features sought, the optimal formulation seems to be S10B5, having contents of 10 wt% silica and 5 wt% barium titanate fillers.

Acknowledgements The research presented in this paper is developed in the context of the project PolyWEC (www.polywec.org, Project Ref. 309139), a FET-Energy project that is partially funded by the 7th Framework Programme of European Community and co-financed by the Romanian National Authority for Scientific Research, CNCS-UEFISCDI (Contract 205EU). One of the authors (C.-D. Varganici) acknowledges the financial support of a grant from the Romanian National Authority for Scientific Research, CNCS-UEFISCDI, Project Number PN-II-ID-PCCE-2011-2-0028.

References

1. Lin Z-H, Yang Y, Wu JM et al (2012) $BaTiO_3$ nanotubes-based flexible and transparent nanogenerators. J Phys Chem Lett 3:3599–3604. doi:10.1021/jz301805f
2. Il Park K, Xu S, Liu Y et al (2010) Piezoelectric $BaTiO_3$ thin film nanogenerator on plastic substrates. Nano Lett 10:4939–4943. doi:10.1021/nl102959k
3. Maas J, Graf C (2012) Dielectric elastomers for hydro power harvesting. Smart Mater Struct 21:064006. doi:10.1088/0964-1726/21/6/064006
4. Pelrine R, Kornbluh R, Joseph J et al (2000) High-field deformation of elastomeric dielectrics for actuators. Mater Sci Eng C 11:89–100. doi:10.1016/S0928-4931(00)00128-4
5. Carpi F, De Rossi D, Kornbluh R, Pelrine R, Sommer-Larsen P (2008) Dielectric elastomers as electromechanical transducers: fundamentals, materials, devices, models and applications of an emerging electroactive polymer technology. Elsevier, Amsterdam
6. Sabourin CL, Carpenter JC, Leib TK, Spivack JL (1996) Biodegradation of dimethylsilanediol in soils. Appl Environ Microbiol 62:4352–4360

7. Chandrasekhar V (2005) Inorganic and organometallic polymers. Inorg Organomet Polym 13:1–339. doi:10.1007/b137079
8. Mark J (1999) Polymer data handbook. Oxford University Press, New York
9. Gallone G, Carpi F, Galantini F, De Rossi D (2008) Enhancing the dielectric permittivity of elastomers. In: Carpi F, De Rossi D, Kornbluh R, Pelrine R, Sommer-Larsen P (eds) Dielectric elastomers as electromechanical transducers: fundamentals, materials, devices, models and applications of an emerging electroactive polymer technology. Elsevier, Amsterdam
10. Nelson JK, Linhardt RJ, Schadler LS, Hillborg H (2012) Effect of high aspect ratio filler on dielectric properties of polymer composites: a study on barium titanate fibers and graphene platelets. IEEE Trans Dielectr Electr Insul 19:960–967. doi:10.1109/TDEI.2012.6215100
11. Cazacu M, Ignat M, Racles C et al (2013) Well-defined silicone-titania composites with good performances in actuation and energy harvesting. J Compos Mater 48:1533–1545. doi:10.1177/0021998313488148
12. Romasanta LJ, Leret P, Casaban L et al (2012) Towards materials with enhanced electro-mechanical response: $CaCu_3Ti_4O_{12}$–polydimethylsiloxane composites. J Mater Chem 22:24705. doi:10.1039/c2jm34674e
13. Molberg M, Walder C, Opris D et al (2009) Frequency-dependent dielectric and mechanical behavior of elastomers for actuator applications. J Appl Phys 106:054112. doi:10.1063/1.3211957
14. Khastgir D, Adachi K (2000) Rheological and dielectric studies of aggregation of barium titanate particles suspended in polydimethylsiloxane. Polymer 41:6403–6413. doi:10.1016/S0032-3861(99)00840-X
15. Kapustianyk V, Shchur Y, Kityk I et al (2008) Nanocrystals incorporated into the PMMA matrix. J Phys Condens Matter 20:365215. doi:10.1088/0953-8984/20/36/365215
16. Lach G, Laskowski L, Kityk IV et al (2007) Dielectric relaxation of $(N(C_2H_5)_4)_2CoCl_2Br_2$ nanocrystallites incorporated into the PMMA matrix. J Non Cryst Solids 353:4353–4356. doi:10.1016/j.jnoncrysol.2007.01.081
17. Cheng K-C, Lin C-M, Wang S-F et al (2007) Dielectric properties of epoxy resin–barium titanate composites at high frequency. Mater Lett 61:757–760. doi:10.1016/j.matlet.2006.05.061
18. Li YC, Tjong SC, Li RKY (2011) Dielectric properties of binary polyvinylidene fluoride/barium titanate nanocomposites and their nanographite doped hybrids. xPRESSS Polym Lett 5:526–534
19. Hanemann T, Schumacher B (2012) Realization of embedded capacitors using polymer matrix composites with barium titanate as high-k-active filler. Microsyst Technol 18:745–751. doi:10.1007/s00542-012-1458-4
20. Chon J, Ye S, Cha KJ et al (2010) High-dielectric sol-gel hybrid materials containing barium titanate nanoparticles. Chem Mater 22:5445–5452. doi:10.1021/cm100729d
21. Nayak S, Kumar Chaki T, Khastgir D (2012) Development of poly(dimethylsiloxane)/$BaTiO_3$ nanocomposites as dielectric material. Adv Mater Res 622–623:897–900. doi:10.4028/www.scientific.net/AMR.622-623.897
22. Nayak S, Chaki TK, Khastgir D (2014) Development of flexible piezoelectric poly(dimethylsiloxane)–$BaTiO_3$ nanocomposites for electrical energy harvesting. Ind Eng Chem Res 53:14982–14992
23. Salamone JC (2015) Polymeric materials encyclopedia, twelve volume set 084932470X. AbeBooks. http://www.abebooks.com/9780849324703/Polymeric-Materials-Encyclopedia-Twelve-Volume-084932470X/plp. Accessed 20 Jan 2015
24. Warrick EL, Pierce OR, Polmanteer KE, Saam JC (1979) Silicone elastomer developments 1967–1977. Rubber Chem Technol 52:437–525. doi:10.5254/1.3535229
25. Bele A, Cazacu M, Stiubianu G, Vlad S (2014) RSC advances silicone–barium titanate composites with increased electromechanical sensitivity. The effects of fillers morphology. RSC Adv 4:58522–58529. doi:10.1039/C4RA09903F
26. Bele A, Cazacu M, Stiubianu G et al (2015) Composites: Part B polydimethylsiloxane–barium titanate composites: preparation and evaluation of the morphology, moisture, thermal, mechanical and dielectric behavior. Composites B 68:237–245. doi:10.1016/j.compositesb.2014.08.050
27. Racles C, Cazacu M, Fischer B, Opris DM (2013) Synthesis and characterization of silicones containing cyanopropyl groups and their use in dielectric elastomer actuators. Smart Mater Struct 22:104004. doi:10.1088/0964-1726/22/10/104004
28. Cazacu M, Racles C, Zaltariov M-F et al (2013) Electroactive composites based on polydimethylsiloxane and some new metal complexes. Smart Mater Struct 22:104008. doi:10.1088/0964-1726/22/10/104008
29. Liu Y, Liu L, Zhang Z et al (2010) Analysis and manufacture of an energy harvester based on a Mooney-Rivlin-type dielectric elastomer. EPL Europhys Lett 90:36004. doi:10.1209/0295-5075/90/36004
30. Alexandru M, Cazacu M, Nistor A, Musteata VE, Stoica I, Grigoras C, Simionescu BC (2010) Polydimethylsiloxane/silica/titania composites preparedby solvent-free sol-gel technique. J Sol Gel Sci Technol 56:310–319
31. Biggs J, Danielmeier K, Hitzbleck J et al (2013) Electroactive polymers: developments of and perspectives for dielectric elastomers. Angew Chem Int Ed 52:9409–9421. doi:10.1002/anie.201301918
32. Madsen FB, Yu L, Daugaard AE et al (2015) A new soft dielectric silicone elastomer matrix with high mechanical integrity and low losses. RSC Adv 5:10254–10259. doi:10.1039/C4RA13511C
33. Cazacu M, Racles C, Vlad A et al (2009) Silicone-based composite for relining of removable dental prosthesis. J Compos Mater 43:2045–2055. doi:10.1177/0021998309340447
34. Freeman G (1962) Silicones: an introduction TSO their chemistry and applications. Iliffe Book Limited, London
35. Diani J, Fayolle B, Gilormini P (2009) A review on the Mullins effect. Eur Polym J 45:601–612. doi:10.1016/j.eurpolymj.2008.11.017
36. Mallinson LG (2001) Ageing studies and lifetime extension of materials. Kluwer, New York
37. Lu J, Wong CP (2008) Nanoparticle-based high-*k* dielectric composites: opportunities and challenges. In: Morris JE (ed) Nanopackaging: nanotechnologies and electronics packaging. Springer, New York, pp 121–137
38. Ying KL, Hsieh TE (2007) Sintering behaviors and dielectric properties of nanocrystalline barium titanate. Mater Sci Eng B 138:241–245. doi:10.1016/j.mseb.2007.01.002
39. Brosseau C (2006) Modelling and simulation of dielectric heterostructures: a physical survey from an historical perspective. J Phys D 39:1277–1294. doi:10.1088/0022-3727/39/7/S02
40. Yoon DH, Zhang J, Lee BI (2003) Dielectric constant and mixing model of $BaTiO_3$ composite thick films. Mater Res Bull 38:765–772. doi:10.1016/S0025-5408(03)00075-8
41. Bosch S, Ferré-Borrull J, Leinfellner N, Canillas A (2000) Effective dielectric function of mixtures of three or more materials: a numerical procedure for computations. Surf Sci 453:9–17. doi:10.1016/S0039-6028(00)00354-X
42. Lichtenecker K, Rother K (1931) Die Herleitung des logarithmischen Mischungsgesetz es aus allgemeinen Prinzipien der stationären Strömung. Physikalische Zeitschrift 32:255–260
43. Nelson SO (1983) Observations on the density dependence of dielectric properties of particulate materials. J Microw Power 18:143–152
44. Landau L, Lifshitz E (1984) Electrodynamics of continuous media, 2nd edn. Pergamon Press, New York

45. Looyenga H (1965) Dielectric constants of heterogeneous mixtures. Physica 31:401–406. doi:10.1016/0031-8914(65)90045-5
46. Karkkainen KK (2000) Effective permittivity of mixtures: numerical validation by the FDTD method. IEEE Trans Geosci Remote Sens 38:1303–1308. doi:10.1109/36.843023
47. Brosseau C, Quéffélec P, Talbot P (2001) Microwave characterization of filled polymers. J Appl Phys 89:4532–4540. doi:10.1063/1.1343521
48. Gershon D, Calame JP, Birnboim A (2001) Complex permittivity measurements and mixings laws of alumina composites. J Appl Phys 89:8110–8116. doi:10.1063/1.1369400
49. Varganici C-D, Ursache O, Gaina C et al (2012) Studies on new hybrid materials prepared by both Diels-Alder and Michael addition reactions. J Therm Anal Calorim 111:1561–1570. doi:10.1007/s10973-012-2532-y
50. Varganici CD, Rosu L, Rosu D, Simionescu BC (2013) Miscibility studies of some semi-interpenetrating polymer networks based on an aromatic polyurethane and epoxy resin. Composites B 50:273–278. doi:10.1016/j.compositesb.2013.02.005
51. Vera-Graziano R, Hernandez-Sanchez F, Cauich-Rodriguez JV (1995) Study of crosslinking density in polydimethylsiloxane networks by DSC. J Appl Polym Sci 55:1317–1327. doi:10.1002/app.1995.070550905
52. Flory PJ, Rehner J (1943) Statistical mechanics of cross-linked polymer networks II. Swelling. J Chem Phys 11:521. doi:10.1063/1.1723792
53. Yang G, Ren W, Mukherjee BK et al (2006) Transverse strain response of silicone dielectric elastomer actuators. J Adv Sci B 18:166–169. doi:10.2978/jsas.18.166
54. Granstrom J, Feenstra J, Sodano HA, Farinholt K (2007) Energy harvesting from a backpack instrumented with piezoelectric shoulder straps. Smart Mater Struct 16:1810–1820. doi:10.1088/0964-1726/16/5/036
55. Kwon D, Rincon-Mora GA (2009) A rectifier-free piezoelectric energy harvester circuit. In: 2009 IEEE international symposium on circuits and systems, IEEE, pp 1085–1088